Cooling a magnetic resonance force microscope via the dynamical back action of nuclear spins

Ya. S. Greenberg,[1,2] E. Il'ichev,[3] and Franco Nori[1,4]

[1]*Advanced Science Institute, The Institute of Physical and Chemical Research (RIKEN), Wako-shi, Saitama 351-0198, Japan*
[2]*Novosibirsk State Technical University, 20 Karl Marx Avenue, 630092 Novosibirsk, Russia*
[3]*Institute of Photonic Technology, P.O. Box 100239, D-07702 Jena, Germany*
[4]*Department of Physics, Center for Theoretical Physics, and Center for the Study of Complex Systems,*
University of Michigan, Ann Arbor, Michigan 48109-1040, USA

We analyze the back-action influence of nuclear spins on the motion of the cantilever of a magnetic force resonance microscope. We calculate the contribution of nuclear spins to the damping and frequency shift of the cantilever. We show that, at the Rabi frequency, the energy exchange between the cantilever and the spin system cools or heats the cantilever depending on the sign of the high-frequency detuning. We also show that the spin noise leads to a significant damping of the cantilever motion.

I. INTRODUCTION

Magnetic resonance force microscopy (MRFM) is a powerful technique for visualizing subsurface structures[1–5] with three-dimensional spatial resolution of the order of 10 nanometers or less,[6] which is more than two orders of magnitude better than the resolution of conventional high-field magnetic resonance imaging (MRI). The main part of a MRFM device is a nanomechanical resonator or cantilever (see Fig. 1 below), having a fundamental frequency in the range of several kHz. By using MRFM, a significant breakthrough in magnetic resonance detection sensitivity was achieved, resulting in single-electron spin detection[7] with a spatial resolution ~25 nm and substantial progress in nuclear spin detection.[8–12] MRFM has also been proposed as a qubit readout device for spin-based quantum computers.[13,14]

MRFM was initially proposed as a possible means to improve the detection sensitivity to the single spin level.[1] Since then, progress in MRFM and related technologies has attracted broad interest, especially the questions of squeezed states of the cantilever and the collapse of its wave function when both, the spin to be measured and the cantilever, are treated quantum mechanically.[15–19] However, the ultimate goal to detect a single nuclear spin with MRFM is still a challenge. Rough estimates indicate that in order to reach this goal the effective temperature of the MRFM cantilever should be reduced to about 0.1 μK, which corresponds to ~2.5 kHz of the fundamental frequency of the MRFM cantilever.

Numerous experiments on cooling micromechanical resonators via their coupling with different external systems have recently been reported (see, e.g., Ref. 20–24). Experimental results show that a micromechanical resonator can be cooled down to an effective temperature on the order of 0.10 K (Ref. 20) or 5 mK (Ref. 23). However, in order to drive the microresonator to the quantum regime, more effective cooling methods are needed. A promising way would be to cool the microresonator by coupling it to a solid-state quantum electronic circuit. In principle, the effective electronic cooling of the microresonator can be achieved by several means,

including coupling it to an another resonator,[25,26] to a transmission line resonator,[27,28] to a quantum dot,[29] or to an electronic spin,[30] or to superconducting devices.[31–43]

In particular (as shown, e.g., in Refs. 35, 37, 39–42, 44, and 45), an electric resonator circuit weakly coupled to a two-level system (superconducting flux qubit) can be *cooled* by its quantum-dynamical *back action*.

In this paper, we investigate the cooling of a MRFM cantilever via its coupling to nuclear spins. We show that the *back action* of the spin system modifies the equation of motion of the cantilever, providing additional damping and a frequency shift which depends on the properties of the spin system (decoherence rates, damping rates, etc). We investigate the operation modes of the MRFM where the damping is positive and results in a substantial decrease in the effective quality factor of the MRFM cantilever, and thus a significant *cooling* of the cantilever motion.
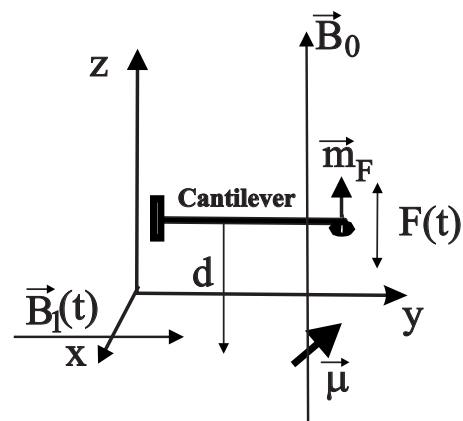

FIG. 1. Schematic diagram of the setup of the system under consideration. Here, B_0 is the uniform permanent magnetic field, $B_1(t)$ is the rotating rf magnetic field, $F(t)$ is an external force acting on the cantilever in the z-direction, m_F is the magnetic moment of the ferromagnetic particle attached to a free end of the cantilever, μ is the magnetic moment of the nuclear spin, located in xy-sample plane, and d is the equilibrium distance between the center of the ferromagnetic particle and a sample plane.

This paper is organized as follows. In Sec. II, we describe the interaction of a MRFM cantilever with nuclear spins. We obtain the cantilever equation of motion modified by the back-action of the spin system. The modification appears as an additional contribution to the damping and frequency shift of the cantilever, in terms of the magnetic spin susceptibility.

In Sec. III, we obtain the explicit expression for the low-frequency spin susceptibility. The most important result of this section is that the *longitudinal* magnetization of a sample has a clear resonance at its Rabi frequency. In some sense, this is the *low-frequency analog of the conventional high-frequency* NMR for the *transverse* magnetization.

Section IV is devoted to a detailed study of the influence of the spin system on the damping and the frequency shift of the cantilever. In the first part of this section we consider a sample with a relative short spin-lattice relaxation time T_1. In this case, we show that the quality factor of the cantilever changes depending on the sign of the high-frequency detuning. For positive detuning (the microwave frequency is above the nuclear resonance frequency), the contribution of the spin system to the cantilever damping is negative: heating the cantilever by absorbing Rabi photons from the spin system. If the detuning is negative (the microwave frequency is below the nuclear resonance frequency), the contribution of the spin system to the cantilever damping is positive: *cooling the cantilever by giving up Rabi photons to the spin system*. In the second part of Sec. IV we consider the influence of the spin noise on the cantilever motion. Independently of the particular values of the parameters which characterize the spin system, we show that its influence on the cantilever damping is always positive, i.e., the spin noise always leads to a decrease of the quality factor of the cantilever.

II. INTERACTION OF NUCLEAR SPINS WITH THE MRFM CANTILEVER

A schematic diagram of the system studied here is shown in Fig. 1. A spherical ferromagnetic particle with magnetic moment m_F is attached to the cantilever tip. A small paramagnetic cluster with magnetic moment μ, which must be detected, is placed on the surface of a nonmagnetic sample beneath the tip of the cantilever. The whole system is placed in a permanent high magnetic field, B_0, oriented in the positive z direction. The transverse magnetic field $B_1(t)$, which excites the NMR in the sample, is applied to the paramagnetic cluster. In addition to B_0, the magnetic moment μ experiences the inhomogeneous field $B_F(z)$ from the ferromagnetic tip. We assume that the field $B_F(z)$ is also oriented in the positive z direction and is given by the dipole formula:

$$B_F(z) = \frac{\mu_0}{4\pi} \frac{2m_F}{(d+z)^3}, \tag{1}$$

where d is the equilibrium distance between the cantilever and the sample surface, and z is the amplitude of the cantilever oscillations. Below we assume $z \ll d$, hence

$$B_F(z) \approx B_F(0)\left(1 - \frac{3}{d}z + \frac{6}{d^2}z^2\right), \tag{2}$$

where

$$B_F(0) = \frac{2\mu_0 m_F}{4\pi d^3}.$$

Hence, the cluster we investigate is under the polarizing field: $B_0 + B_F(0)$.

The interaction of a particle, having a magnetic moment μ, with the cantilever is given by the following Hamiltonian

$$H = H_C + H_C^{(b)} + H_{CB} + H_S + H_S^{(b)} + H_{SB} - (\vec{\mu} \cdot \vec{B}), \tag{3}$$

where H_C is the Hamiltonian of the cantilever

$$H_C = \frac{p^2}{2m} + \frac{m\omega^2 z^2}{2}, \tag{4}$$

H_S is the Hamiltonian of a nuclear spin interacting with a one-mode high-frequency field

$$H_S = \frac{\hbar\omega_0}{2}\sigma_Z + \frac{\hbar\omega_1}{2}\sigma_X(a^+ + a) + \hbar\omega_{\mathrm{mw}}a^+ a, \tag{5}$$

where

$$\omega_0 = \gamma[B_0 + B_F(0)],$$

γ is the nuclear gyromagnetic ratio, ω_{mw} is the frequency of the microwave field. The quantity $\hbar\omega_1$, the interaction energy between spin and the microwave field, is proportional to its amplitude B_1 (see below). The magnetic moment $\vec{\mu}$ of a spin-1/2 particle is expressed in terms of the Pauli spin matrix vector: $\vec{\mu} = -\hbar\gamma\vec{\sigma}/2$.

The Hamiltonians $H_C^{(b)}$ and $H_S^{(b)}$ represent the thermal baths for the cantilever and spin, respectively, while H_{CB} and H_{SB} represent their interactions with their corresponding baths.

We will not specify here the bath Hamiltonians $H_C^{(b)}$, $H_S^{(b)}$, their interactions H_{CB}, and H_{SB}. We describe the influence of H_C and H_{CB} on the motion of the cantilever by introducing the damping rate γ_c and the external noise $\eta(t)$.

We consider the cantilever tip as an oscillator with effective mass m, and effective spring constant k_s, subject to an external force $F_0 \cos \omega t$ and force fluctuations with a spectral density

$$S_F(\omega) = 2\hbar\omega \frac{m\omega_c}{Q_c}\coth\left(\frac{\hbar\omega}{2kT}\right), \tag{6}$$

where Q_c is the quality factor of the bare cantilever.

The equation of motion for the cantilever, interacting with N spin-1/2 particles, then reads:

$$\ddot{z} + \gamma_c\dot{z} + \omega_c^2 z = \left\langle \frac{\hat{M}_Z}{m}\frac{dB_F}{dz} \right\rangle + f_0\cos\nu t + \eta(t), \tag{7}$$

where $\hat{M}_Z$ is the quantum operator of the longitudinal magnetization,

$$\hat{M}_Z = -\frac{N\hbar\gamma}{2}\sigma_Z,$$

$\omega_c = (k_s/m)^{1/2}$, $\gamma_c = \omega_c/Q_c$, $f_0 = F_0/m$, and $\eta(t)$ describes the fluctuations of the acceleration, and has a spectral density $S_\eta(\omega) = S_F(\omega)/m^2$.

By using Eq. (2) we obtain:

$$\left\langle \frac{\hat{M}_Z}{m}\frac{dB_F}{dz}\right\rangle = \lambda\langle\sigma_Z\rangle - \frac{4\lambda}{d}\langle z\sigma_Z\rangle, \qquad (8)$$

where

$$\lambda = \frac{3N\hbar\gamma B_F(0)}{2md}$$

is the coupling strength between the spin and the cantilever. The angular brackets in Eqs. (7) and (8) denote the average over the two free baths variables.

The quantity $\langle\sigma_Z\rangle$ in Eq. (8) is a functional of the cantilever position $z(t)$, where its first order $(\approx z/d)$ contribution to the Hamiltonian Eq. (3) is $(\lambda m z + f)\sigma_Z$, where we introduce $f(t)$: a small external force that is required for calculating the magnetic susceptibility.[46] Hence, to first order in λ, we obtain

$$\langle\sigma_Z(t)\rangle = \langle\sigma_Z^{(0)}(t)\rangle + \lambda m \int dt_1 \frac{\delta\langle\sigma_Z(t)\rangle}{\delta f(t_1)}z(t_1), \qquad (9)$$

where $\langle\sigma_Z^{(0)}(t)\rangle$ is described by the evolution of the spin system $(H_S + H_S^{(b)} + H_{SB})$ uncoupled from the cantilever.

The functional derivative $\delta\langle\sigma_Z(t)\rangle/\delta f(t_1)$ in Eq. (9) is the response of the spin system to the weak low-frequency external force $f(t)$. It has the magnetic susceptibility $\chi_{zz}(\omega)$ of the spin system as its Fourier transform:

$$\frac{\delta\langle\sigma_Z(t)\rangle}{\delta f(t_1)} = \int \frac{d\omega}{2\pi}\exp[-i\omega(t-t_1)]\chi_{zz}(\omega), \qquad (10)$$

From Eqs. (9) and (8) we obtain the equation of motion of the cantilever:

$$\ddot{z} + \gamma_c\dot{z} + \omega_c^2 z = \lambda\langle\sigma_Z^{(0)}(t)\rangle - \frac{4\lambda}{d}\langle\sigma_Z^{(0)}(t)\rangle z$$
$$+ \lambda^2 m \int dt_1 \frac{\delta\langle\sigma_Z(t)\rangle}{\delta f(t_1)}z(t_1) + f_0\cos\nu t + \eta(t). \qquad (11)$$

Let us now analyze this equation in detail. The first two terms in the right-hand side of Eq. (11) contribute, respectively, to the amplitude and the frequency shifts due to the spins. The modulation of either of these terms is usually employed in MRFM experiments. In particular, the second term of the right-hand side of Eq. (11) can be easily converted to the frequently used expression for the frequency shift:[12]

$$\Delta f = m_z f_c (d^2 B_z/dz^2)/2k_c,$$

where m_z is the magnetic moment of the sample. These two terms describe the direct influence of the spin on cantilever motion.

The third term in the right-hand side of Eq. (11) describes the *additional back-action of the spin on the cantilever motion*, which is due to the modification of the spin dynamics by the cantilever. This term, which is the main subject of our study here, gives rise to an additional frequency shift and an additional damping of the cantilever.

Assuming that the steady-state value of the quantity $\langle\sigma_Z^{(0)}(t)\rangle$ is independent of time, we convert Eq. (11) to Fourier components of $z(t)$ [using $z(t) = \int e^{-i\omega t}z(\omega)d\omega$]:

$$\left\{\omega_c^2 - \omega^2 + \frac{4\lambda}{d}\langle\sigma_Z^{(0)}\rangle - \lambda^2 m\chi_{zz}'(\omega)\right.$$
$$\left. - i[\omega\gamma_c + \lambda^2 m\chi_{zz}''(\omega)]\right\}z(\omega)$$
$$= \frac{f_0}{2}\delta(\omega-\nu) + \eta(\omega), \qquad (12)$$

where we introduce the real and imaginary parts of the spin susceptibility

$$\chi_{zz}(\omega) = \chi_{zz}'(\omega) + i\chi_{zz}''(\omega).$$

Analyzing the third and the fourth terms of the rhs of Eq. (12) we see that the influence of the spins on the cantilever produces the frequency shift

$$\Delta\omega = \frac{2\lambda}{d\omega_c}\langle\sigma_Z^{(0)}\rangle - \frac{\lambda^2 m\chi_{zz}'(\omega)}{2\omega_c}, \qquad (13)$$

where the first term in the rhs of Eq. (13) represents the *direct* contribution of the spins to the frequency shift, while the second term in the rhs of Eq. (13) is the additional contribution to the frequency shift that results from the *indirect* influence of the back-action of the spins on the cantilever motion.

From the fifth term in the rhs of Eq. (12), $-i[\omega\gamma_c + \lambda^2 m\chi_{zz}''(\omega)]z(\omega)$, we can write the total damping of the cantilever:

$$\gamma_{\text{total}} = \gamma_c + \gamma_{\text{spin}}, \qquad (14)$$

where γ_{spin} is the frequency-dependent contribution of the back-action of the spins to the damping of the cantilever:

$$\gamma_{\text{spin}} = \frac{\lambda^2 m\chi_{zz}''(\omega)}{\omega}. \qquad (15)$$

From this expression we obtain a spin back-action-induced modification of the cantilever quality factor:

$$\frac{1}{Q} = \frac{1}{Q_c} + \frac{\lambda^2 m\chi_{zz}''(\omega)}{\omega_c^2}. \qquad (16)$$

III. LOW-FREQUENCY MAGNETIC SUSCEPTIBILITY OF IRRADIATED SPINS

The interaction of a two level system with an external electromagnetic field tuned near the resonance of this two-level system can be described using the dressed-state approach,[47] which recently was successfully applied to in-

vestigate the interaction between solid state superconducting qubits and an external radiation source.[41,48] Some results obtained in Ref. [41] within the dressed-state approach will be applied here for the investigation of the interaction of a MRFM cantilever with irradiated nuclear spins.

The energy levels of a spin-1/2 interacting with a high-frequency ω_{mw} field has a term proportional[47] to the number N_{ph} of photons, with an additional splitting of each photon state by the Rabi energy $\hbar\Omega_R/2$:

$$E^{\pm}(N_{ph}) = \hbar\omega_{mw}N_{ph} \pm \frac{1}{2}\hbar\Omega_R, \qquad (17)$$

where Ω_R is the Rabi frequency

$$\Omega_R = \sqrt{\delta^2 + \Omega_1^2}, \qquad (18)$$

with

$$\Omega_1 = \omega_1\langle N_{ph}\rangle^{1/2};$$

where $\langle N_{ph}\rangle$ is the average number of high-frequency photons,[49] and

$$\delta = \omega_{mw} - \omega_0$$

is the high-frequency detuning. For definitiveness, here we assume $\delta > 0$. The frequency Ω_1 is directly related to the amplitude of microwave field: $\Omega_1 = \gamma B_1$.

As was shown in Ref. [41], this system can be described, within the RWA approach, by the rate equations for the elements of the reduced density matrix, which describe the transition between Rabi levels [the levels $E^{\pm}(N_{ph})$ in Eq. (17), with the same N_{ph}].

$$\frac{d\rho}{dt} = -A_1\rho + B\rho_+ + (\Gamma_-)\cos 2\theta, \qquad (19)$$

$$\frac{d\rho_+}{dt} = -i\Omega_R\rho_- + B\rho - A_2\rho_+ + (\Gamma_-)\sin 2\theta, \qquad (20)$$

$$\frac{d\rho_-}{dt} = -i\Omega_R\rho_+ - \Gamma_\varphi\rho_-, \qquad (21)$$

where

$$A_1 = \left[\frac{1}{T_1}\cos^2 2\theta + \Gamma_\varphi \sin^2 2\theta\right], \qquad (22)$$

$$A_2 = \left[\frac{1}{T_1}\sin^2 2\theta + \Gamma_\varphi \cos^2 2\theta\right], \qquad (23)$$

$$B = \left[\Gamma_\varphi - \frac{1}{T_1}\right]\sin 2\theta \cos 2\theta, \qquad (24)$$

where Γ_φ is the dephasing rate of a spin, which can be expressed in terms of the spin-spin relaxation time T_2, $\Gamma_\varphi = 1/T_2$. Here, T_1 is the spin-lattice relaxation time, which is related to up $\Gamma_\uparrow$ and down $\Gamma_\downarrow$ transition rates between spin levels

$$T_1^{-1} = \Gamma_\uparrow + \Gamma_\downarrow; \quad \Gamma_- = \Gamma_\uparrow - \Gamma_\downarrow.$$

The angle θ is defined by $\tan 2\theta = -\Omega_1/\delta$, where $0 < 2\theta < \pi$, so that

$$\cos 2\theta = -\delta/\Omega_R,$$

and

$$\cos\theta = \frac{1}{\sqrt{2}}\left(1 - \frac{\delta}{\Omega_R}\right)^{1/2}; \quad \sin\theta = \frac{1}{\sqrt{2}}\left(1 + \frac{\delta}{\Omega_R}\right)^{1/2}$$

For equilibrium conditions, the relaxation $\Gamma_\downarrow$ and excitation $\Gamma_\uparrow$ rates are related by the detailed balance law:

$$\Gamma_\uparrow = \Gamma_\downarrow\exp\left(-\frac{\hbar\omega_0}{k_BT}\right). \qquad (25)$$

From Eq. (25) we obtain

$$T_1\Gamma_- = -\tanh\left(\frac{\hbar\omega_0}{2k_BT}\right). \qquad (26)$$

The quantity ρ in Eq. (19) is defined as the difference of the populations between the higher and the lower Rabi levels.

The steady-state solution $\left(\frac{d\rho}{dt} = \frac{d\rho_-}{dt} = \frac{d\rho_+}{dt} = 0\right)$ for Eqs. (19)–(21) is as follows:

$$\rho^{(0)} = \frac{(\Gamma_\varphi^2 + \Omega_R^2)}{\frac{\Gamma_\varphi^2}{T_1} + A_1\Omega_R^2}(\Gamma_-)\cos 2\theta, \qquad (27)$$

$$\rho_+^{(0)} = \frac{\Gamma_\varphi^2}{\frac{\Gamma_\varphi^2}{T_1} + A_1\Omega_R^2}(\Gamma_-)\sin 2\theta, \qquad (28)$$

$$\rho_-^{(0)} = -i\frac{\Omega_R}{\Gamma_\varphi}\rho_+^{(0)}. \qquad (29)$$

It is interesting to note that under high-frequency irradiation, the population of the Rabi levels becomes inverted. This is seen from Eq. (27), where the quantity $\rho^{(0)}$ is positive, since for $\delta > 0$ we have $\cos 2\theta = -\delta/\Omega_R < 0$, and always $\Gamma_- < 0$.

In addition, as δ tends to zero, $\rho^{(0)} \to 0$, which causes the equalization of the population of the two levels when the high frequency irradiation is in exact resonance with the NMR frequency γB_0.

The quantity $\langle\sigma_Z(t)\rangle$ which is, by definition, the longitudinal magnetization of a sample with N spin-1/2 particles (see Appendix A) can be expressed[41] in terms of the matrix elements ρ and ρ_+:

$$\langle\sigma_Z(t)\rangle = \rho(t)\cos 2\theta + \rho_+(t)\sin 2\theta. \qquad (30)$$

Therefore, from the definition of $\chi_{zz}(\omega)$ in Eq. (10) we obtain

$$\chi_{zz}(\omega) = \chi_\rho(\omega)\cos 2\theta + \chi_{\rho_+}(\omega)\sin 2\theta, \qquad (31)$$

where $\chi_\rho(\omega)$ and $\chi_{\rho_+}(\omega)$ are the spectral components of the response of $\rho(t)$ and $\rho_+(t)$ to a weak external force, and are defined similarly to Eq. (10).

The susceptibilities $\chi_\rho(\omega)$ and $\chi_{\rho_+}(\omega)$ can be readily found by investigating the response of the reduced density matrix

in Eqs. (19)–(21) to a weak external perturbation [see Eqs. (B8)–(B10) in Appendix B]. Hence, the expression for $\chi_{zz}(\omega)$ becomes:

$$\chi_{zz}(\omega) = \frac{\delta\Omega_1\Omega_R}{\hbar D(\omega)\Gamma_\varphi^2}\rho_+^{(0)}(-i\omega + 2\Gamma_\varphi), \qquad (32)$$

where $D(\omega)$ is given in Eq. (B11).

The quantity $\rho_+^{(0)}$ in Eq. (32) is the steady-state value [Eq. (28)] which can be written as follows:

$$\rho_+^{(0)} = -\frac{\Omega_1}{\Omega_R}\frac{1}{1 + (\delta T_2)^2 + T_2 T_1 \Omega_1^2}\tanh\left(\frac{\hbar\omega_0}{2k_B T}\right), \qquad (33)$$

and can be expressed in terms of the stationary magnetization Eq. (A10):

$$\frac{N\hbar\gamma}{2}\rho_+^{(0)} = -\frac{M_Z^{(\text{st})}}{1 + (\delta T_2)^2}\frac{\Omega_1}{\Omega_R}. \qquad (34)$$

Resonance of the longitudinal magnetization at the Rabi frequency

Historically, the detection of NMR is based on the Faraday law of induction.[50] That is why most of the measurement schemes in NMR are based on the detection of the *transverse* magnetization, which oscillates with a relatively high frequency.

The detection of the *longitudinal* magnetization is less common because it requires measurements in a low frequency range with a low signal-to-noise ratio. However, this drawback can be circumvented by some techniques, such as the prepolarization of a sample in high field,[51] or the use of superconducting quantum interference devices (SQUIDs),[52] which allow to obtain, in the micro and nano-Tesla range, a resolution which is beyond what is usually achieved in conventional high-field NMR.[53–57]

In MRFM there is no choice other than to measure the longitudinal component of the nuclear polarization, since the resonance frequencies of MRFM cantilevers are well below those corresponding to the frequencies of NMR transitions. From this point of view, it is interesting to note that the *longitudinal* magnetization M_z of a sample placed in a high frequency resonant radiation field *shows a clear resonance at the Rabi frequency if the sample is subject to an additional low-frequency excitation* directed along the z axis with energy (see Fig. 2)

$$H_{\text{LF}} = \hbar\gamma B_2 \cos\omega t.$$

As shown in Refs. 41 and 58, this effect is a general feature of any two-level dissipative system. In this case, the low-frequency evolution of the longitudinal magnetization can be expressed in terms of the spin susceptibility $\chi_{zz}(\omega)$ Eq. (32):

$$M_Z(t) = M_Z^{(\text{st})} + \frac{N\hbar\gamma}{2}\hbar\gamma B_2[\chi_{zz}'(\omega)\cos\omega t + \chi_{zz}''(\omega)\sin\omega t], \qquad (35)$$
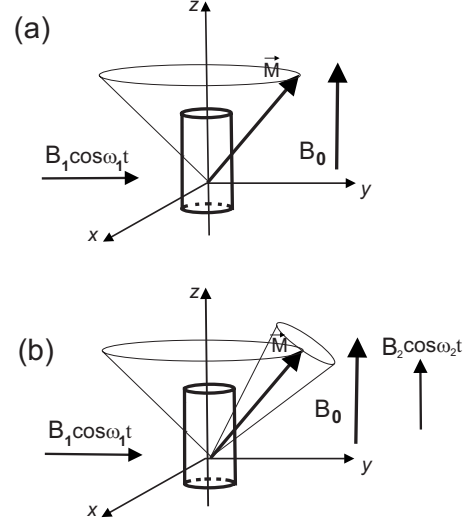
where $M_Z^{(\text{st})}$ is given by Eq. (A10).

FIG. 2. Resonance of the longitudinal magnetization M_z at the Rabi frequency Ω_R. (a) For conventional NMR, the longitudinal magnetization of a sample polarized in the field B_0 and subject to a circularly polarized excitation field $B_1 \cos\omega_1 t$, where $\omega_1 \approx \omega_0$, exhibits a precession around the z-axis with a time-independent steady-state z projection of the longitudinal magnetization M_z. (b) A second low-frequency excitation $B_2 \cos\omega_2 t$, where $\omega_2 \approx \Omega_R$, applied along the z axis, produces resonant oscillations of M_z near the Rabi frequency Ω_R.

With the aid of Eq. (34) we rewrite Eq. (35) in the following form:

$$M_Z(t) = M_Z^{(\text{st})}\left\{1 + \frac{B_2}{B_1}[\tilde{\chi}_{zz}'(\omega)\cos\omega t + \tilde{\chi}_{zz}''(\omega)\sin\omega t]\right\}, \qquad (36)$$

where

$$\tilde{\chi}_{zz}'(\omega) = -\frac{\delta\Omega_1^3(-i\omega + 2\Gamma_\varphi)}{D(\omega)\Gamma_\varphi^2[1 + (T_2\delta)^2]},$$

$$T_2 = 1/\Gamma_\varphi, \quad \Omega_1 = \gamma B_1, \qquad (37)$$

B_1 is the amplitude of the *high*-frequency resonance excitation, and B_2 is the amplitude of the *low*-frequency signal, which excites the Rabi oscillations of the longitudinal magnetization M_z.

The resonance at the Rabi frequency Ω_R is clearly seen in Fig. 3, where we plot (for two values of the spin-spin relaxation time T_2) the dissipative part of the spin susceptibility Eq. (37) as a function of the low-frequency $\omega(\omega \approx \Omega_R)$.

It should be remembered that our linear approximation is valid within the range

$$\frac{N\hbar\gamma}{2}\hbar\gamma B_2|\chi_{zz}(\omega)| < M_Z^{(\text{st})}, \qquad (38)$$

from where we obtain the range of the amplitudes of the low-frequency signal B_2, where the expression Eq. (36) is consistent with the condition Eq. (38):

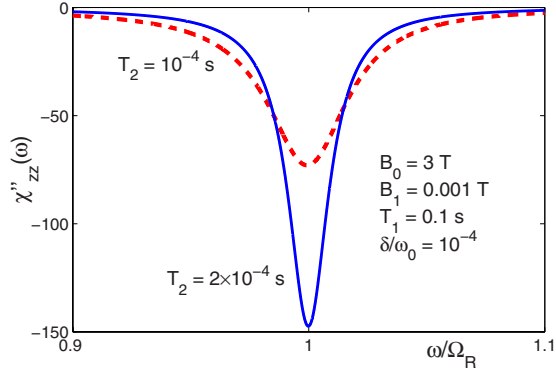$$B_2 < B_1/\tilde{\chi}_{zz,\text{max}}''(\omega).$$

FIG. 3. (Color online) The dependence of dissipative part $\tilde{\chi}''_{zz}(\omega)$ of spin susceptibility for low frequencies $\omega \approx \Omega_R$.

Hence, *near the Rabi resonance* (*i.e.*, $\omega \approx \Omega_R$), a significant modulation of the longitudinal magnetization M_z can be induced by a low-frequency drive.

The resonance of the longitudinal magnetization described above is, in some sense, a *low-frequency analog of conventional NMR*, where the resonance of the transverse nuclear magnetization is being measured at a high resonance frequency.

IV. INFLUENCE OF SPINS ON THE FREQUENCY SHIFT AND THE DAMPING OF THE CANTILEVER

A. Influence of the driven equilibrium longitudinal magnetization on the damping and frequency shift of the cantilever

Here, we consider the situation where, before the measurements start, the spins under the application of a polarizing external magnetic field reach thermal equilibrium with their environment. In other words, in this case, the spin-lattice relaxation time T_1 is sufficiently short (for example, in the millisecond range) to ensure the application of conventional NMR measurement protocols. For this case, the corresponding susceptibilities are given by the expressions Eqs. (B12)–(B14).

In order to analyze the damping and the frequency shift of the cantilever in Eq. (12), we explicitly write down the real and imaginary parts of $\chi_{zz}(\omega)$ from Eq. (32):

$$\chi'_{zz}(\omega) = \frac{\delta \Omega_1 \Omega_R}{\hbar \Gamma_\varphi^2} \rho_+^{(0)} \frac{2\Gamma_\varphi D_1(\omega) - \omega D_2(\omega)}{D_1^2(\omega) + D_2^2(\omega)}, \quad (39)$$

$$\chi''_{zz}(\omega) = -\frac{\delta \Omega_1 \Omega_R}{\hbar \Gamma_\varphi^2} \rho_+^{(0)} \frac{\omega D_1(\omega) + 2\Gamma_\varphi D_2(\omega)}{D_1^2(\omega) + D_2^2(\omega)}, \quad (40)$$

where

$$D_1(\omega) \equiv \mathrm{Re}[D(\omega)] = \frac{1}{T_1}[A_1 T_1 \Omega_R^2 + \Gamma_\varphi^2 - \omega^2(1 + 2T_1\Gamma_\varphi)], \quad (41)$$

$$D_2(\omega) \equiv \mathrm{Im}[D(\omega)] = \omega\left(\omega^2 - \Omega_R^2 - \Gamma_\varphi^2 - \frac{2\Gamma_\varphi}{T_1}\right). \quad (42)$$

It is worth noting that at the exact resonance ($\delta = 0$), the back-action influence of the spins on the cantilever vanishes, since the corresponding susceptibilities Eq. (39) and (40) are equal to zero at this point. This is a consequence of the equalization of the population of Rabi levels at the point of exact resonance ($\rho^{(0)}$ tends to zero as δ approaches zero). This produces the *vanishing of the energy flow between the spins and the cantilever at the Rabi frequency.*

Another point is that the sign of the susceptibility $\chi''_{zz}(\omega)$ in Eq. (40) is *opposite* to that of δ, for any value of its parameters. This follows from the fact that the numerator $\omega D_1(\omega) + 2\Gamma_\varphi D_2(\omega)$ in Eq. (40) is always negative, and the quantity $\rho_+^{(0)}$ is also negative. Therefore, for $\delta > 0$ (when the higher Rabi level is more populated than the lower) the contribution of the spins to the damping of the cantilever is negative [see Eq. (12)]. In this case, *the cantilever is being heated by absorbing the Rabi photons emitted by the spins.*

In the opposite case, when $\delta < 0$ (i.e., the higher Rabi level is less populated than the lower) the contribution of the spins to the damping of the cantilever is positive, therefore *cooling the cantilever, which gives up Rabi photons to the spin system.*

It is worthwhile to consider the dependence of the dissipative part of susceptibility $\chi''_{zz}(\omega)$ [Eq. (40)] on the frequency ω. It has two peaks. A Lorentzian peak is in the vicinity of the Rabi frequency Ω_R, as it is evident from Eq. (42). The condition for this is the relative large high-frequency detuning ($\delta \gg \Gamma_\varphi, \Omega_1$). The approximate expression for the peak value at the Rabi resonance is as follows:

$$\chi''_{zz}(\omega)|_{\mathrm{peak}} \approx \rho_+^{(0)} \frac{\delta \Omega_1}{2\hbar \Gamma_\varphi^3} \quad (43)$$

The other peak is related to the spin-lattice relaxation time T_1 of the longitudinal magnetization. It lies at much lower frequencies ($\omega \ll \Omega_R$). If we assume $\omega \ll \Omega_R, \Gamma_\varphi$; $\delta \gg \Gamma_\varphi, T_1, \Omega_1$; $\Gamma_\varphi T_1 \gg 1$, we obtain $D_1(\omega) \approx \delta^2/T_1$, $D_2(\omega) \approx -\delta^2\omega$, which yields the following expressions for the susceptibility:

$$\chi'_{zz}(\omega) \approx \rho_+^{(0)} \frac{\delta}{|\delta|} \frac{2\Omega_1 T_1}{\hbar \Gamma_\varphi} \frac{1}{1 + \omega^2 T_1^2} \quad (44)$$

$$\chi''_{zz}(\omega) \approx \rho_+^{(0)} \frac{\delta}{|\delta|} \frac{2\Omega_1 T_1}{\hbar \Gamma_\varphi} \frac{\omega T_1}{1 + \omega^2 T_1^2} \quad (45)$$

with the maximum of $\chi''_{zz}(\omega)$ being at $\omega_{\mathrm{max}} = 1/T_1$. These expressions are analogous to the Debye formulas for the low-frequency dispersion of the dielectric constant. In the context of NMR, this Debye-like behavior is known for the response of the transverse magnetization in a weak polarizing field.[59]

To estimate the magnitude of this effect, we take as a guide the experimentally accessible parameters from Ref. 12. From Fig. 2(b) of that paper we take the following values of the magnetic field $B_F(0)$ on the tip, $B_F(0) = 100$ mT, and a corresponding value of d, the distance between the tip and the sample: $d = 60$ nm. From the spring constant $k_c = 6$
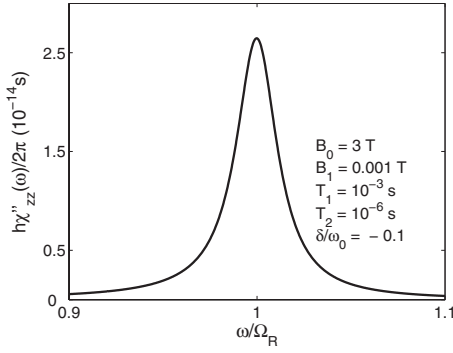
FIG. 4. The imaginary part of spin susceptibility as function of normalized frequency ω/Ω_R in the vicinity of Rabi frequency, for $T = 0.6$ K, $N = 10^5$.

$\times 10^{-5}$ N/m and the resonance frequency of the cantilever, $f_c = 3$ kHz, we estimate the cantilever mass

$$m = k_c/\omega_c^2 = 1.6 \times 10^{-13} \text{ kg}.$$

For the element ^{19}F, which was the subject of study in Ref. 12, the nuclear gyromagnetic ratio $\gamma = 2\pi \times 40$ MHz/T. This allows to estimate the coupling factor λ:

$$\lambda = \frac{3N\hbar\gamma B_F(0)}{2md} \approx (4.12 \times 10^{-7} \times N)\frac{m}{s^2}.$$

Here N is the number of spins in the resonant slice. Thus, for the factor $\lambda^2 m/\hbar$ we obtain the estimate

$$\frac{\lambda^2 m}{\hbar} \approx (2.6 \times 10^8 \times N^2) \text{ s}^{-3}.$$

In addition, we take $T_1 = 10^{-3}$ s, $T_2 = 1/\Gamma_\varphi = 10^{-6}$ s, $T = 0.6$ K, $B_0 = 3$ T, and $B_1 = \Omega_1/\gamma = 10^{-3}$ T.

The contribution of the spins to the cantilever *damping* γ_{spin} is proportional to the imaginary part of the spin system susceptibility $\chi_{zz}''(\omega)$ [see Eq. (15)]. The susceptibility $\chi_{zz}''(\omega)$ has a clear resonance at the Rabi frequencies, which is shown in Fig. 4. The second Debye-like peak is shown in Fig. 5. It is worthwhile to note that for the parameters we used here the peak value in Fig. 5 is much higher than the Rabi peak in Fig. 4.
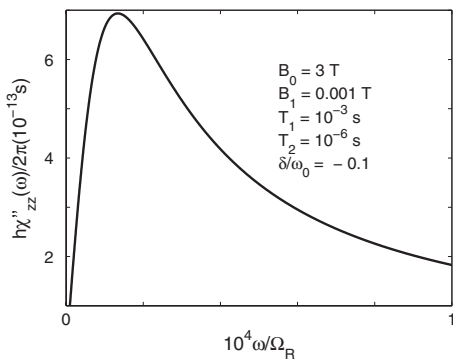

FIG. 5. The imaginary part of spin susceptibility as a function of the normalized frequency ω/Ω_R, in the vicinity of the Debye-like peak, for $T = 0.6$ K, and $N = 10^5$.
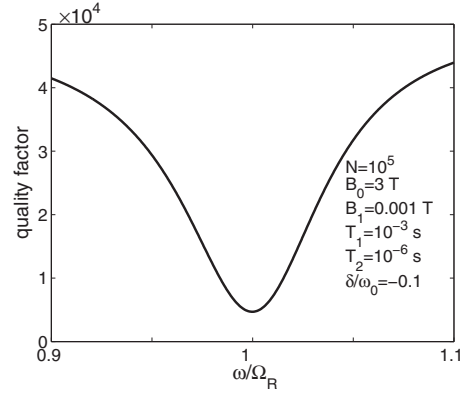

FIG. 6. The modified quality factor Q of the cantilever near the Rabi frequency Ω_R. Here, the quality factor of the unloaded cantilever is $Q_c = 5 \times 10^4$, $T = 0.6$ K.

These resonances modify within the corresponding frequency range the bare cantilever quality factor Q_c in Eq. (16), as shown in Fig. 6 and Fig. 7.

The contribution to the cantilever *frequency shift* is given by the real part of the spin system susceptibility $\chi_{zz}'(\omega)$ in Eq. (39). The associated frequency shift, $\lambda^2 m\chi_{zz}'(\omega)/2\omega_c$, near the Rabi resonance is shown in Fig. 8, and near the Debye-like peak in Fig. 9.

For the parameters used here, the Rabi frequency $\Omega_R \approx 12$ MHz and the Debye-like peak in Fig. 5 is located near 160 Hz. Between these two peaks, the quality factor is gradually increased from about 200 to almost its bare value of 50 000 before it falls down to 5000 at the Rabi frequency. The resonance frequency of the cantilever ($f_c = 3$ KHz) lies at the continuation of the right side of the curve shown in Fig. 7. The calculations show that at $f = 3$ KHz the quality factor $Q \approx 1,800$ with the frequency shift $\Delta f \approx 0.32$ Hz, which is in the range of the modified bandwidth (≈ 2 Hz). In principle, the dissipative part of the susceptibility $\chi_{zz}''(\omega)$ is very sensitive to its parameters, especially, to δ, Γ_φ, and Ω_1. If we had taken, for example, $T_2 = 1/\Gamma_\varphi = 10^{-7}$ s, other parameters being unchanged, we would obtain $Q \approx 200$ near 3 kHz, the resonance of the cantilever. Hence, while in the real experiment the external parameters, such as δ and Ω_1 can be controlled, the estimation of the damping effect at the given frequency requires the knowledge, with good accuracy, of the spin-spin relaxation time T_2.
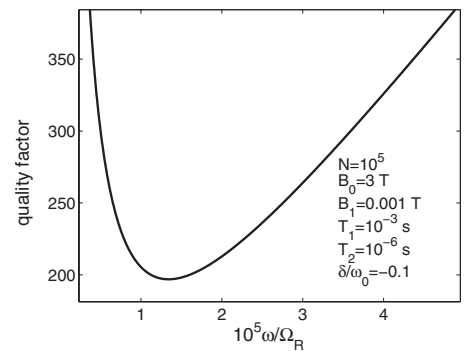

FIG. 7. The modified quality factor Q of the cantilever near the Debye-like peak. Here, the quality factor Q_c of the unloaded cantilever is $Q_c = 5 \times 10^4$, and $T = 0.6$ K.
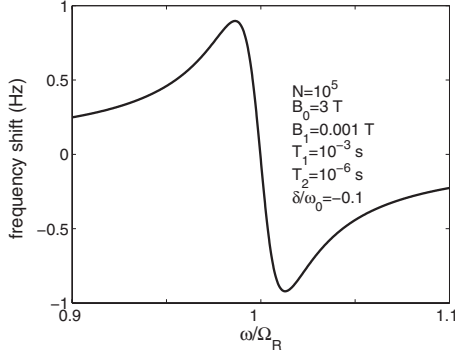
FIG. 8. Frequency shift, $\lambda^2 m \chi'_{zz}(\omega)/2\omega_c$, due to the back-action of the spins, versus the normalized frequency ω/Ω_R, for $T=0.6$ K.

B. Effect of the nuclear spin noise on the damping of the cantilever

If the spin-lattice relaxation time T_1 is extremely long, which happens at low temperatures, it is not possible to use conventional NMR methods, which rely on the measurement of the equilibrium spin polarization. In addition, for nano-scale volumes (below about $(100 \text{ nm})^3$) the statistical spin polarization exceeds the mean Boltzmann polarization.[60] Hence, an alternative approach would be to measure a naturally-occurring statistical polarization: the spin noise.[6,12,61] In this case, a sample has a magnetic moment with a mean-squared-value proportional to $\sqrt{N}\mu$, where N is the number of nuclear spins in the resonant slice, and μ is the magnetic moment of a single particle.[60,62]

Hence, for long T_1 we take for $\rho(t')$, $\rho_+(t')$, and $\rho_-(t')$, in Eqs. (B8)–(B10) their *initial* values: $\rho(0)$, $\rho_+(0)$, and $\rho_-(0)$. These values correspond to natural spin fluctuations in a sample which is in thermal equilibrium and under no external influence ($\omega_0=0$, $\Omega_1=0$). In order to find $\rho(0)$, $\rho_+(0)$, and $\rho_-(0)$, we put $\Omega_1=0$ in Eqs. (27)–(29). In this case the Rabi levels disappear and we get a sample in a constant polarizing field B_0 with $\rho^{(0)}=-T_1\Gamma_-$, the equilibrium normalized population difference between two levels [see Eq. (26)]. Hence, for this case, the quantity $\rho^{(0)}$, which before was the population difference between Rabi levels, remains the population difference between levels of a spin in the field B_0. Therefore, in the absence of an e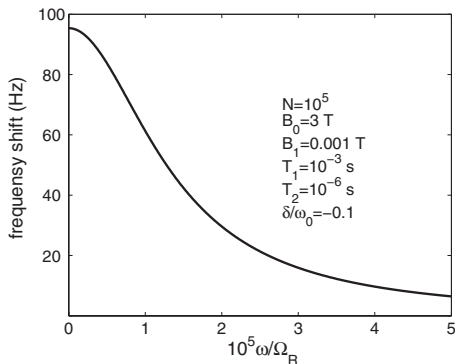xternal field ($B_0=0$) it is reasonable to consider $\rho^{(0)}$ as $\rho(0)$, the apparent normalized population difference which provides the mean-squared value of the naturally occurring magnetic moment $\sqrt{N}\mu$. Hence,

$$\rho(0) = -\frac{\sqrt{N}\mu}{N\mu} = -\frac{1}{\sqrt{N}}$$

Here, the quantity $\rho(0)$ is negative because the upper level is now less populated than the lower one.

In the same limit ($\Omega_1=0$) we obtain from Eqs. (28) and (29) $\rho_+^{(0)}=\rho_-^{(0)}=0$. This result does not depend on B_0 and remains unchanged when $B_0=0$. The quantities $\rho_+^{(0)}$ and $\rho_-^{(0)}$ describe the density matrix elements between Rabi levels (see Eqs. (26) in Ref. 41), which should tend to zero when Rabi levels disappear. Hence, in the absence of the polarizing field B_0, it is reasonable to consider $\rho_+^{(0)}=\rho_+(0)=0$ and $\rho_-^{(0)}=\rho_-(0)=0$.

Therefore, for the corresponding susceptibilities, we obtain the expressions Eqs. (B15)–(B17). Hence, in this case the expression for $\chi_{zz}(\omega)$ becomes:

$$\chi_{zz}(\omega) = \frac{\Omega_1^2}{\hbar\sqrt{N}\Omega_R d(\omega)}\left[\frac{\Gamma_\varphi \Omega_1^2}{\Omega_R^2} - i\left(\omega - \frac{\delta^2 \Gamma_\varphi}{\Omega_R^2}\right)\right], \quad (46)$$

where $d(\omega)$ is given in Eq. (B18).

The use of the spin noise for the MRFM 2D and 3D image reconstruction of the nuclear spin density was described in Refs. 6 and 12. These papers briefly reported that they measured an unexplained substantial decrease of the quality factor of the cantilever (from 50 000 to 8000 in Ref. 12, and from 30 000 to several thousand in Ref. 6). Here, we show that, qualitatively, *this effect might be explained by the back action of spin noise on the cantilever motion.*

For the quantitative estimate of this effect, we take as a guide the necessary parameters from Ref. 12. Here, we now assume that the spin-lattice relaxation time T_1 is so long that it prevents the manipulation of the equilibrium Boltzmann polarization. For example, for the atom ^{19}F in calcium fluoride CaF_2 studied in Ref. 12, the time T_1 at the experimental[63] temperature $T=0.6$ K was about 10^4 s.

The investigation of the imaginary part of the magnetic susceptibility Eq. (46) shows that its dependence on the high-frequency detuning δ shows a sharp peak at the point of resonance, $\delta=0$ (see Fig. 10, where the function $\chi''_{zz}(\omega)$ is drawn at the resonance of the cantilever). Thus, we now write down the real and imaginary parts of the magnetic susceptibility Eq. (46) for the exact resonance ($\delta=0$), where we expect the maximum effect:

$$\chi'_{zz}(\omega) = -\frac{\Omega_1}{\hbar\sqrt{N}|d(\omega)|^2}(\omega^2-\Omega_1^2)(\omega^2+\Gamma_\varphi^2), \quad (47)$$

$$\chi''_{zz}(\omega) = \frac{\omega\Omega_1\Gamma_\varphi}{\hbar\sqrt{N}|d(\omega)|^2}(\omega^2+\Gamma_\varphi^2), \quad (48)$$

and here

$$|d(\omega)|^2 = \omega^2(\omega^2-\Omega_1^2-\Gamma_\varphi^2)^2 + \Gamma_\varphi^2(\Omega_1^2-2\omega^2)^2. \quad (49)$$
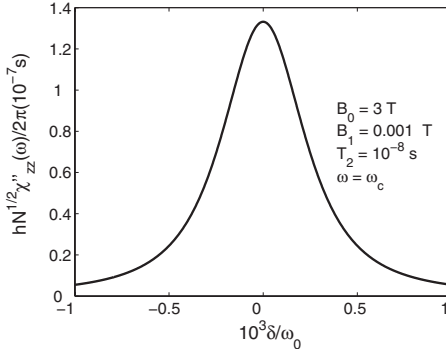

FIG. 9. Frequency shift, $\lambda^2 m \chi'_{zz}(\omega)/2\omega_c$, near the Debye-like peak, for $T=0.6$ K.

FIG. 10. The dependence of the dissipative part of the spin susceptibility on the high frequency detuning $\delta = \omega_{\mathrm{mw}} - \omega_0$, with $\omega_c / 2\pi = 3$ kHz.

FIG. 11. The dependence of the dissipative part of the spin susceptibility on the distance x from the point of exact resonance, and here $\omega_c / 2\pi = 3$ kHz.

From Eq. (48) it follows that the contribution of the spins to the damping of the cantilever is always positive, which means that the spin noise is cooling the cantilever.

The width of the distribution $\Delta \delta$ shown in Fig. 10 is directly connected to the thickness of the resonant slice $\Delta x = \Delta \delta / \gamma G$, where G is the magnetic field gradient. The dependence of the dissipative part of the spin susceptibility on the distance from the point of exact resonance is shown in Fig. 11 for $B_0 = 3$ T and $G = 1.5 \times 10^6$ T/m. From this figure, we estimate the effective thickness of the resonant slice as the full-width at half-maximum of the curve shown in Fig. 11. Thus, we obtain $\Delta x \approx 1$ nm, which corresponds to the width of high-frequency detuning $\Delta \delta \approx 5 \times 10^{-4} \omega_0$ (The full-width at half-maximum of the curve in Fig. 10).

For example, if we take for the sample the dimensions $90 \times 90 \times 80$ nm^3, with roughly 30 million nuclear spins (see Ref. 12), we obtain the effective number of spins in the resonant slice $90 \times 90 \times 1$ nm^3 that gives the main contribution to the effect: $N_{\mathrm{eff}} \approx 3.5 \times 10^5$.

Below we estimate, from Eq. (48), the contribution of the spin noise to the cantilever damping at the resonance frequency of the cantilever ω_c, assuming $\Gamma_\varphi \gg \omega / 2\pi, \Omega_1 / 2\pi$. The result is (see Eq. (16)):

$$\frac{\lambda^2 m \chi_{zz}''(\omega)}{\omega_c^2} = \frac{\lambda^2 m}{\sqrt{N} \hbar \omega_c^2 \Gamma_\varphi} \frac{\Omega_1}{\omega_c}. \tag{50}$$

In order to estimate the modified quality factor from Eq. (50), we take $N \approx 10^5$, the number of spins in the resonant slice, $\Gamma_\varphi \approx 10^8$ s^{-1}, $f_c = 3$ kHz, and the bare $Q_c = 5 \times 10^4$. Hence, for zero high-frequency detuning ($\delta = 0$) we obtain from Eq. (16) the modified quality factor $Q \approx 0.3$. This enormous reduction of the quality factor is primarily due to the large number of nuclei N, which are simultaneously at the exact magnetic resonance ($\delta = 0$).

However, we stress that, strictly speaking, our estimates above cannot be considered as the only possible explanation of the cantilever damping observed in Refs. 6 and 12. One of the reasons for this is that the long side of the cantilever in Refs. 6 and 12 was perpendicular to the sample surface, which is different from the design shown in Fig. 1. For their design, the damping of the cantilever due to the spin-noise back-action is more sensitive (compared to our case) to the
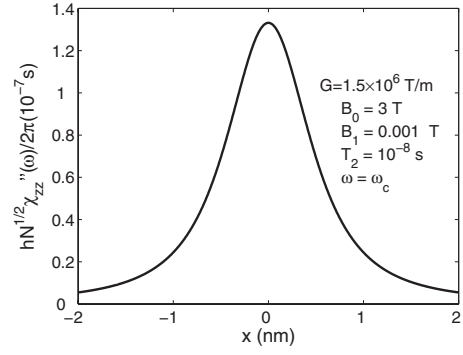
density distribution of the spins over the sample surface. Another reason is that here we assume that all resonant spins feel the same field and are located at the same distance from the tip just beneath it. Hence, to obtain more realistic values of Q, it is necessary to modify Eq. (1) with a more careful account of the density distribution of the resonant spins over a sample.

V. CONCLUSION

In this paper, we investigate the interaction of the MRFM cantilever with a system of nuclear spins. We show that the back action of nuclear spins results in an additional contribution to the damping and frequency shift of the cantilever vibrations. We also show that a spin system may significantly change the quality factor of the cantilever. The cantilever can be either heated or cooled, depending on the sign of the high-frequency detuning. This effect exhibits a resonant nature, with a maximum at the Rabi frequency. We show that the main reason for this effect is that the longitudinal magnetization (which is commonly measured in MRFM experiments) exhibits a resonance at the Rabi frequency, which can significantly alter its low-frequency evolution. We also analyze the influence of the spin noise on the cantilever damping and show that the spin noise may lead to a significant reduction of the quality factor of the cantilever.

The interesting question is the lower bound on the cooling of the cantilever by nuclear spins. It might seem at first that the lower limit on the cooling of the cantilever is set by its zero-point fluctuations. However, this is not the case. From general considerations, the lower limit is set by the direct contribution of the spin noise to the cantilever fluctuations (see, for example, Ref. 25). In order to make a reasonable estimate of this limiting temperature, it is necessary to: a) first calculate the spectrum of the spin fluctuations under a high-frequency field, and b) afterwards to consider a small number of Rabi photons, which requires treating the cantilever quantum mechanically. In our paper, we treat the spin system quantum mechanically, while the number of Rabi photons is large, which means that the cantilever behaves classically. This problem will be the subject of future investigations.

APPENDIX A: DYNAMICS OF AN IRRADIATED SPIN IN THE DRESSED STATE APPROACH

Here, we very briefly summarize some results of Ref. 41, as applied to the problem we study in this paper.

In addition to Eqs. (19)–(21) (which describe the transition between Rabi levels of an irradiated spin) the (spin +field) system can also be characterized by the density matrix elements κ's which describe the transitions between levels with photon numbers that differ by one. These levels are approximately separated by $\hbar\omega_0$, the energy between the levels of a bare spin. The rate equations for the κ's are:[41]

$$\frac{d\kappa^+}{dt} = -i\omega_{mw}\kappa^+, \tag{A1}$$

$$\frac{d\kappa}{dt} = -i\omega_{mw}\kappa - A_1\kappa + B\kappa_+ + \kappa^+(\Gamma_-)\cos 2\theta, \tag{A2}$$

$$\frac{d\kappa_+}{dt} = -i\omega_{mw}\kappa_+ - i\Omega_R\kappa_- + B\kappa - A_2\kappa_+ + \kappa^+(\Gamma_-)\sin 2\theta, \tag{A3}$$

$$\frac{d\kappa_-}{dt} = -i\omega_{mw}\kappa_- - i\Omega_R\kappa_+ - \Gamma_\varphi\kappa_-. \tag{A4}$$

For possible applications of this method, the quantities to be measured are the averages of the Pauli spin operators $\langle\sigma_X\rangle$, $\langle\sigma_Y\rangle$, and $\langle\sigma_Z\rangle$. As was shown in Ref. 41

$$\langle\sigma_Z\rangle = \rho(t)\cos 2\theta + \rho_+(t)\sin 2\theta, \tag{A5}$$

$$\langle\sigma_X\rangle = \sin 2\theta \, \mathrm{Re}[\kappa(t)] - \cos 2\theta \, \mathrm{Re}[\kappa_+(t)] - \mathrm{Re}[\kappa_-(t)], \tag{A6}$$

$$\langle\sigma_Y\rangle = -\sin 2\theta \, \mathrm{Im}[\kappa(t)] + \cos 2\theta \, \mathrm{Im}[\kappa_+(t)] + \mathrm{Im}[\kappa_-(t)]. \tag{A7}$$

These quantities are directly connected to the longitudinal magnetization of a sample with N spin-1/2 particles:

$$M_Z = -\frac{N\gamma\hbar}{2}\langle\sigma_Z\rangle, \tag{A8}$$

and its transverse components

$$M_X = -\frac{N\gamma\hbar}{2}\langle\sigma_X\rangle; \quad M_Y = -\frac{N\gamma\hbar}{2}\langle\sigma_Y\rangle. \tag{A9}$$

It is very instructive here to show that the steady-state solution for the density matrix provides the well-known Bloch expressions for the longitudinal and transverse components of the magnetization.

The stationary magnetization $M_Z^{(st)}$, which is defined in Eq. (A8), is obtained from Eq. (30) with the help of Eqs. (27) and (28). By using the substitutions $\Gamma_\varphi = 1/T_2$, $\Omega_1 = \gamma B_1$, we obtain for $M_Z^{(st)}$:

$$M_Z^{(st)} = M_0 \frac{1 + (T_2\delta)^2}{1 + (T_2\delta)^2 + T_1T_2(\gamma B_1)^2}, \tag{A10}$$

where

$$M_0 = \frac{N\hbar\gamma}{2}\tanh\left(\frac{\hbar\gamma B_0}{2k_BT}\right).$$

Now we find the steady-state solutions of Eqs. (A1)–(A4). It is not difficult to see that the solution of these equations has the form: $\kappa^+ = c^+e^{-i\omega_{mw}t}$, $\kappa = ce^{-i\omega_{mw}t}$, $\kappa_+ = c_+e^{-i\omega_{mw}t}$, $\kappa_- = c_-e^{-i\omega_{mw}t}$, where

$$c = c^+\frac{\Gamma_-}{D}(\Gamma_\varphi^2 + \Omega_R^2)\cos 2\theta, \tag{A11}$$

$$c_+ = c^+\frac{\Gamma_-}{D}\Gamma_\varphi^2\sin 2\theta, \tag{A12}$$

$$c_- = -ic^+\frac{\Gamma_-}{D}\Omega_R\Gamma_\varphi\sin 2\theta, \tag{A13}$$

$$D = \frac{\Gamma_\varphi^2 + \delta^2}{T_1} + \Gamma_\varphi\Omega_1^2. \tag{A14}$$

By choosing $c^+ = 1$ and using Eqs. (A6) and (A7) to calculate Eq. (A9) we find

$$M_x = M_c \cos\omega_{mw}t + M_s\sin\omega_{mw}t, \tag{A15}$$

$$M_y = -M_s\cos\omega_{mw}t + M_c\sin\omega_{mw}t, \tag{A16}$$

where

$$M_c = M_0\frac{T_2^2\delta\gamma B_1}{1 + (T_2\delta)^2 + T_1T_2(\gamma B_1)^2}, \tag{A17}$$

$$M_s = M_0\frac{T_2\gamma B_1}{1 + (T_2\delta)^2 + T_1T_2(\gamma B_1)^2}. \tag{A18}$$

Therefore, the steady-state solution of the density matrix Eqs. (19)–(21) and (A1)–(A4) provides the well known expressions for the longitudinal Eq. (A10) and transverse components Eqs. (A17) and (A18) of the magnetization.[59]

APPENDIX B: LOW-FREQUENCY RESPONSE OF AN IRRADIATED TWO-LEVEL SYSTEM

The response of a two-level system to a weak external force $f(t)$, in the limit of vanishing force $f(t)$, is found from the following equations:

$$\frac{d\rho}{dt} = -A_1\rho + B\rho_+ - \frac{i}{\hbar}f(t)\rho_-\sin 2\theta + (\Gamma_-)\cos 2\theta, \quad (B1)$$

$$\frac{d\rho_+}{dt} = -i\Omega_R\rho_- + B\rho - A_2\rho_+ + \frac{i}{\hbar}f(t)\rho_-\cos 2\theta + (\Gamma_-)\sin 2\theta, \quad (B2)$$

$$\frac{d\rho_-}{dt} = -i\Omega_R\rho_+ - \Gamma_\varphi\rho_- + \frac{i}{\hbar}f(t)(\rho_+\cos 2\theta - \rho\sin 2\theta). \quad (B3)$$

By taking the functional derivative with respect to $f(t')$ we obtain

$$\left(\frac{d}{dt} + A_1\right)\frac{\delta\rho(t)}{\delta f(t')} - B\frac{\delta\rho_+(t)}{\delta f(t')} = -\frac{i}{\hbar}\delta(t-t')\rho_-(t')\sin 2\theta \quad (B4)$$

$$\left(\frac{d}{dt} + A_2\right)\frac{\delta\rho_+(t)}{\delta f(t')} - B\frac{\delta\rho(t)}{\delta f(t')} + i\Omega_R\frac{\delta\rho_-(t)}{\delta f(t')}$$
$$= \frac{i}{\hbar}\delta(t-t')\rho_-(t')\cos 2\theta, \quad (B5)$$

$$\left(\frac{d}{dt} + \Gamma_\varphi\right)\frac{\delta\rho_-(t)}{\delta f(t')} + i\Omega_R\frac{\delta\rho_+(t)}{\delta f(t')}$$
$$= \frac{i}{\hbar}\delta(t-t')[\rho_+(t')\cos 2\theta - \rho(t')\sin 2\theta], \quad (B6)$$

where we used the definition $\delta f(t)/\delta f(t') = \delta(t-t')$.

The corresponding susceptibilities $\chi_\rho(\omega)$, $\chi_{\rho_+}(\omega)$, $\chi_{\rho_-}(\omega)$ are defined similar to Eq. (10):

$$\frac{\delta\rho(t)}{\delta f(t')} = \int\frac{d\omega}{2\pi}\exp^{-i\omega(t-t')}\chi_\rho(\omega), \text{etc.} \quad (B7)$$

From Eqs. (B4)–(B6) we can readily find the susceptibilities $\chi_\rho(\omega)$, $\chi_{\rho_+}(\omega)$, and $\chi_{\rho_-}(\omega)$:

$$\chi_\rho(\omega) = -\frac{i}{\hbar D(\omega)}\left\{\rho_-(t')\sin 2\theta\left[(-i\omega + \Gamma_\varphi)\left(-i\omega + \frac{1}{T_1}\right)\right.\right.$$
$$\left.\left. + \Omega_R^2\right] - \Omega_R B[\rho_+(t')\cos 2\theta - \rho(t')\sin 2\theta]\right\}, \quad (B8)$$

$$\chi_{\rho_+}(\omega) = \frac{i}{\hbar D(\omega)}\{\rho_-(t')\cos 2\theta(-i\omega + \Gamma_\varphi)(-i\omega + A_1)$$
$$- \rho_-(t')\sin 2\theta B(-i\omega + \Gamma_\varphi) - i\Omega_R[\rho_+(t')\cos 2\theta$$
$$- \rho(t')\sin 2\theta](-i\omega + A_1)\}, \quad (B9)$$

$$\chi_{\rho_-}(\omega) = \frac{i}{\hbar D(\omega)}\left(-i\omega + \frac{1}{T_1}\right)\{(-i\omega + \Gamma_\varphi)[\rho_+(t')\cos 2\theta$$
$$- \rho(t')\sin 2\theta] - i\Omega_R\rho_-(t')\cos 2\theta\}, \quad (B10)$$

where

$$D(\omega) = (-i\omega + \Gamma_\varphi)^2\left(-i\omega + \frac{1}{T_1}\right) + (-i\omega + A_1)\Omega_R^2. \quad (B11)$$

The functional derivatives Eq. (B7) are defined for $t > t'$, where t' is the time the external force is being applied. Hence, the susceptibilities Eqs. (B8)–(B10) describe the evolution of the system for times $t > t'$, with the $\rho(t')$'s, corresponding to when the external force is applied. Therefore, the subsequent evolution of the system depends on its state just before the perturbation is applied.

In what follows we consider two cases. The first one is when the relaxation time T_1 is relatively short. In this case the system quickly reaches thermal equilibrium during the measurement. For this case, we take for $\rho(t')$, $\rho_+(t')$, and $\rho_-(t')$, their steady-state values: $\rho^{(0)}$ from Eq. (27), $\rho_+^{(0)}$ from Eq. (28), and $\rho_-^{(0)}$ from Eq. (29). For the corresponding susceptibilities, we obtain the following expressions:[41]

$$\chi_\rho(\omega) = -\frac{\Omega_R}{\hbar D(\omega)\Gamma_\varphi}\rho_+^{(0)}\left\{\sin 2\theta\left[(-i\omega + \Gamma_\varphi)\left(-i\omega + \frac{1}{T_1}\right)\right.\right.$$
$$\left.\left. + \Omega_R^2\right] + \frac{\Omega_R^2}{\Gamma_\varphi}B\cos 2\theta\right\}, \quad (B12)$$

$$\chi_{\rho_+}(\omega) = \frac{\Omega_R}{\hbar D(\omega)\Gamma_\varphi}\cos 2\theta\rho_+^{(0)}\left[(-i\omega + \Gamma_\varphi)\left(-i\omega + \frac{1}{T_1}\right)\right.$$
$$\left. - (-i\omega + A_1)\frac{\Omega_R^2}{\Gamma_\varphi}\right], \quad (B13)$$

$$\chi_{\rho_-}(\omega) = i\frac{\Omega_R^2}{\hbar D(\omega)\Gamma_\varphi^2}\rho_+^{(0)}\cos 2\theta\left(-i\omega + \frac{1}{T_1}\right)(-i\omega + 2\Gamma_\varphi). \quad (B14)$$

The other case is when the spin-lattice relaxation time T_1 is extremely long compared to the measurement time. If we measure the spin noise in this case, then it is reasonable to take $\rho(0) = -1/\sqrt{N}$, $\rho(0)_+ = \rho(0)_- = 0$ (see the explanation in Sec. III). For the corresponding susceptibilities, we obtain from Eq. (B8)–(B10) (in the limit $1/T_1 \ll \omega$):

$$\chi_\rho(\omega) = -\frac{i\delta\Omega_1^2\Gamma_\varphi}{\hbar\sqrt{N}d(\omega)\Omega_R^2}, \quad (B15)$$

$$\chi_{\rho_+}(\omega) = \frac{\Omega_1}{\hbar\sqrt{N}d(\omega)}\left(-i\omega + \Gamma_\varphi\frac{\Omega_1^2}{\Omega_R^2}\right), \quad (B16)$$

$$\chi_{\rho_-}(\omega) = \frac{\omega\Omega_1}{\hbar\sqrt{N}d(\omega)\Omega_R}(-i\omega + \Gamma_\varphi), \quad (B17)$$

where

$$d(\omega) = \Gamma_\varphi(\Omega_1^2 - 2\omega^2) + i\omega(\omega^2 - \Omega_R^2 - \Gamma_\varphi^2). \quad (B18)$$

[1] J. A. Sidles, J. L. Garbini, K. J. Bruland, D. Rugar, O. Züger, S. Hoen, and C. S. Yannoni, Rev. Mod. Phys. **67**, 249 (1995).

[2] A. Suter, Prog. Nucl. Magn. Reson. Spectrosc. **45**, 239 (2004).

[3] S. Kuehn, S. A. Hickman, and J. A. Marohn, J. Chem. Phys. **128**, 052208 (2008).

[4] P. C. Hammel and D. V. Pelekhov, in *Handbook of Magnetism and Advanced Magnetic Materials*, edited by H. Kronmüller and S. Parkin (Wiley, New York, 2007), Vol. 5.

[5] P. C. Hammel, D. V. Pelekhov, P. E. Wigen, T. R. Gosnell, M. M. Midzor, and M. L. Roukes, Proc. IEEE **91**, 789 (2003).

[6] C. L. Degen, M. Poggio, H. J. Mamin, C. T. Rettner, and D. Rugar, Proc. Natl. Acad. Sci. U.S.A. **106**, 1313 (2009).

[7] D. Rugar, R. Budakian, H. J. Mamin, and B. W. Chui, Nature (London) **430**, 329 (2004).

[8] D. Rugar, O. Züger, S. Hoen, C. S. Yannoni, H.-M. Vieth, and R. D. Kendrick, Science **264**, 1560 (1994).

[9] K. R. Thurber, L. E. Harrel, and D. D. Smith, J. Magn. Reson. **162**, 336 (2003).

[10] K. R. Thurber, L. E. Harrel, R. Fainchtein, and D. D. Smith, Appl. Phys. Lett. **80**, 1794 (2002).

[11] H. J. Mamin, R. Budakian, B. W. Chui, and D. Rugar, Phys. Rev. B **72**, 024413 (2005).

[12] H. J. Mamin, M. Poggio, C. L. Degen, and D. Rugar, Nat. Nanotechnol. **2**, 301 (2007).

[13] G. P. Berman, G. D. Doolen, P. C. Hammel, and V. I. Tsifrinovich, Phys. Rev. B **61**, 14694 (2000).

[14] D. V. Pelekhov, I. Martin, A. Suter, D. V. Reagor, and P. C. Hammel, Proc. SPIE **4656**, 1 (2002).

[15] F. Xue, L. Zhong, Y. Li, and C. P. Sun, Phys. Rev. B **75**, 033407 (2007).

[16] F. Xue, Y. X. Liu, C. P. Sun, and F. Nori, Phys. Rev. B **76**, 064305 (2007).

[17] H. Gassmann, M.-S. Choi, H. Yi, and C. Bruder, Phys. Rev. B **69**, 115419 (2004).

[18] G. P. Berman, F. Borgonovi, G. Chapline, S. A. Gurvitz, P. C. Hammel, D. V. Pelekhov, A. Suter, and V. I. Tsifrinovich, J. Phys. A **36**, 4417 (2003).

[19] G. P. Berman, F. Borgonovi, H.-S. Goan, S. A. Gurvitz, and V. I. Tsifrinovich, Phys. Rev. B **67**, 094425 (2003).

[20] D. Kleckner and D. Bouwmeester, Nature (London) **444**, 75 (2006).

[21] C. H. Metzger and K. Karrai, Nature (London) **432**, 1002 (2004).

[22] J. D. Teufel, C. A. Regal, and K. W. Lehnert, New J. Phys. **10**, 095002 (2008).

[23] M. Poggio, C. L. Degen, H. J. Mamin, and D. Rugar, Phys. Rev. Lett. **99**, 017201 (2007).

[24] A. Schliesser, P. Del'Haye, N. Nooshi, K. J. Vahala, and T. J. Kippenberg, Phys. Rev. Lett. **97**, 243905 (2006).

[25] M. Grajcar, S. Ashhab, J. R. Johansson, and F. Nori, Phys. Rev. B **78**, 035406 (2008).

[26] K. R. Brown, J. Britton, R. J. Epstein, J. Chiaverini, D. Leibfried, and D. J. Wineland, Phys. Rev. Lett. **99**, 137205 (2007).

[27] J. Zhang, Y. X. Liu, and F. Nori, Phys. Rev. A **79**, 052102 (2009).

[28] F. Xue, Y. D. Wang, Y. X. Liu, and F. Nori, Phys. Rev. B **76**, 205302 (2007).

[29] S.-H. Ouyang, J. Q. You, and F. Nori, Phys. Rev. B **79**, 075304 (2009).

[30] P. Rabl, P. Cappellaro, M. V. Gurudev Dutt, L. Jiang, J. R. Maze, and M. D. Lukin, Phys. Rev. B **79**, 041302(R) (2009).

[31] A. Naik, O. Buu, M. D. LaHaye, A. D. Armour, A. A. Clerk, M. P. Blencowe, and K. C. Schwab, Nature (London) **443**, 193 (2006).

[32] I. Martin, A. Shnirman, L. Tian, and P. Zoller, Phys. Rev. B **69**, 125339 (2004).

[33] M. P. Blencowe, J. Imbers, and A. D. Armour, New J. Phys. **7**, 236 (2005).

[34] A. A. Clerk and S. Bennett, New J. Phys. **7**, 238 (2005).

[35] E. Il'ichev, N. Oukhanski, A. Izmalkov, Th. Wagner, M. Grajcar, H.-G. Meyer, A. Yu. Smirnov, A. Maassen van den Brink, M. H. S. Amin, and A. M. Zagoskin, Phys. Rev. Lett. **91**, 097906 (2003).

[36] F. Nori, Nat. Phys. **4**, 589 (2008).

[37] M. Grajcar, S. H. W. Van der Ploeg, A. Izmalkov, E. Il'ichev, H.-G. Meyer, A. Fedorov, A. Shnirman, and G. Schön, Nat. Phys. **4**, 612 (2008).

[38] S. O. Valenzuela, W. D. Oliver, D. M. Berns, K. K. Berggren, L. S. Levitov, and T. P. Orlando, Science **314**, 1589 (2006).

[39] J. Hauss, A. Fedorov, S. Andre, V. Brosco, C. Hutter, R. Kothari, S. Yeshwanth, A. Shnirman, and G. Schön, New J. Phys. **10**, 095018 (2008).

[40] J. Hauss, A. Fedorov, C. Hutter, A. Shnirman, and G. Schön, Phys. Rev. Lett. **100**, 037003 (2008).

[41] Ya. S. Greenberg, Phys. Rev. B **76**, 104520 (2007).

[42] Ya. S. Greenberg and E. Il'ichev, Phys. Rev. B **77**, 094513 (2008).

[43] J. Q. You, Y. X. Liu, and F. Nori, Phys. Rev. Lett. **100**, 047001 (2008).

[44] J. Q. You, Y. X. Liu, C. P. Sun, and F. Nori, Phys. Rev. B **75**, 104516 (2007).

[45] S. Ashhab, J. R. Johansson, A. M. Zagoskin, and F. Nori, New J. Phys. **11**, 023030 (2009).

[46] A. Yu. Smirnov, Phys. Rev. B **68**, 134514 (2003).

[47] C. Cohen-Tannoudji, J. Dupont-Roc, and G. Grynberg, *Atom-Photon Interactions. Basic Processes and Applications* (Wiley, New York, 1998).

[48] Y. X. Liu, C. P. Sun, and F. Nori, Phys. Rev. A **74**, 052321 (2006).

[49] The substitution of the actual photon number N_{ph} by its average value $\langle N_{ph} \rangle$ means that we treat the driving field classical. In this sence, the Eqs. (19)–(21) describe the evolution of Rabi levels originated from the interaction of two-level system with a classical (coherent state) driving field.

[50] M. Packard and R. Varian, Phys. Rev. **93**, 941 (1954).

[51] S. Appelt, F. W. Hasing, H. Kuhn, J. Perlo, and B. Blumich, Phys. Rev. Lett. **94**, 197602 (2005).

[52] Ya. S. Greenberg, Rev. Mod. Phys. **70**, 175 (1998).

[53] R. McDermott, S. K. Lee, B. ten Haken, A. H. Trabesinger, A. Pines, and J. Clarke, Proc. Natl. Acad. Sci. U.S.A. **101**, 7857 (2004).

[54] R. McDermott, A. H. Trabesinger, M. Mück, E. L. Hahn, A. Pines, and J. Clarke, Science **295**, 2247 (2002).

[55] V. S. Zotev, P. L. Volegov, A. N. Matlashov, M. A. Espy, J. C. Mosher, and R. H. Kraus, Jr., J. Magn. Reson. **192**, 197 (2008).

[56] V. S. Zotev, A. N. Matlashov, P. L. Volegov, I. M. Savukov, M. A. Espy, J. C. Mosher, J. J. Gomez, and R. H. Kraus, Jr., J. Magn. Reson. **194**, 115 (2008).

[57] M. Burghoff, S. Hartwig, and L. Trahms, Appl. Phys. Lett. **87**, 054103 (2005).

[58] Ya. S. Greenberg, E. Il'ichev, and A. Izmalkov, Europhys. Lett. **72**, 880 (2005).

[59] A. Abragam, *The Principles of Nuclear Magnetism* (Clarendon Press, Oxford, 1961).

[60] C. L. Degen, M. Poggio, H. J. Mamin, and D. Rugar, Phys. Rev. Lett. **99**, 250601 (2007).

[61] H. J. Mamin, R. Budakian, B. W. Chui, and D. Rugar, Phys. Rev. Lett. **91**, 207604 (2003).

[62] F. Bloch, Phys. Rev. **70**, 460 (1946).

[63] P. L. Kuhns, P. C. Hammel, O. Gonen, and J. S. Waugh, Phys. Rev. B **35**, 4591 (1987).